

Intracellular Drug Delivery Nanocarriers of Glutathione-Responsive Degradable Block Copolymers Having Pendant Disulfide Linkages

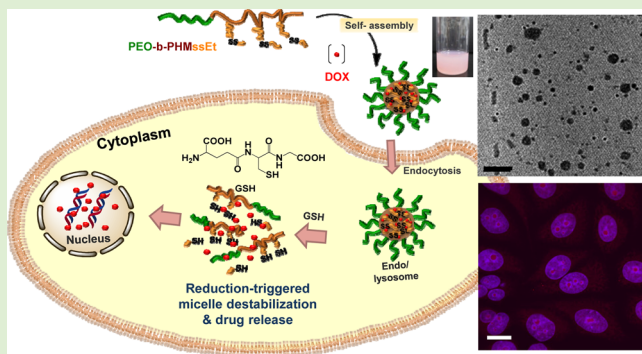
Behnoush Khorsand,[†] Gabriel Lapointe,[‡] Christopher Brett,[‡] and Jung Kwon Oh*,[†]

[†]Department of Chemistry and Biochemistry and Center for Nanoscience Research, Concordia University, Montreal, Quebec, Canada H4B 1R6

[‡]Department of Biology, Concordia University, Montreal, Quebec, Canada H4B 1R6

Supporting Information

ABSTRACT: Self-assembled micelles of amphiphilic block copolymers (ABPs) with stimuli-responsive degradation (SRD) properties have a great promise as nanotherapeutics exhibiting enhanced release of encapsulated therapeutics into targeted cells. Here, thiol-responsive degradable micelles based on a new ABP consisting of a pendant disulfide-labeled methacrylate polymer block (PHMssEt) and a hydrophilic poly(ethylene oxide) (PEO) block were investigated as effective intracellular nanocarriers of anticancer drugs. In response to glutathione (GSH) as a cellular trigger, the cleavage of pendant disulfide linkages in hydrophobic PHMssEt blocks of micellar cores caused the destabilization of self-assembled micelles due to change in hydrophobic/hydrophilic balance. Such GSH-triggered micellar destabilization changed their size distribution with an appearance of large aggregates and led to enhanced release of encapsulated anticancer drugs. Cell culture results from flow cytometry and confocal laser scanning microscopy for cellular uptake as well as cell viability measurements for high anticancer efficacy suggest that new GSH-responsive degradable PEO-b-PHMssEt micelles offer versatility in multifunctional drug delivery applications.



INTRODUCTION

Polymer-based drug delivery systems (polymer-DDSs) are promising platforms in biotechnology, biomedicine, and pharmaceutical science, because they enable enhancing therapeutic efficacy and thus reducing side effects common to small drugs.^{1–5} In particular, self-assembled micellar aggregates based on amphiphilic block copolymers (ABPs) consist of hydrophobic cores, enabling encapsulation of hydrophobic biomolecules, surrounded with hydrophilic coronas, ensuring biocompatibility and aqueous colloidal stability.^{6–8} In the design of multifunctional micellar aggregates as effective polymer-DDSs, a challenge to be addressed is the controlled and enhanced release of encapsulated drugs in targeted diseased cells, particularly cancer cells. Diffusion-controlled release through nanopores of micellar cores as a passive method, flow-controlled release by variation of osmotic pressure, and swelling-controlled release by volume change have been utilized. However, these methods exhibit several drawbacks; they include difficult control of release rate, limited selection of polymers to be thermoresponsive, or requirements for cross-linking reactions.⁹ The promising method is stimuli-responsive degradation (SRD) of covalent bonds in micelles that are cleaved in controllable and tunable response to external stimuli;^{10,11} thus, SRD enables the enhanced release of encapsulated therapeutics into targeted cells while facilitating the removal of empty vehicles after the release.^{12–15}

Furthermore, this platform has been explored for tuning lower critical solution temperature (LCST) of polymeric materials,^{16–19} changing morphologies of self-assembled nanostructures,^{20–22} and fabricating highly ordered nanoporous films.^{23–25}

Typical external stimuli include oxidative,²⁶ enzymatic reaction,²⁷ low pH,^{28–32} light,^{33–35} ultrasound,^{36,37} and glucose.^{38,39} Reductive reaction employing disulfide-thiol chemistry is particularly promising because disulfide linkages are cleaved to the corresponding thiols in response to thiols or reducing agents.^{40,41} In biological systems, glutathione (GSH reduced form, a tripeptide containing cysteine) having a pendant sulphydryl (–SH) groups as a cellular reducing agent is found at different concentrations in intracellular (≈ 10 mM) and extracellular compartments ($< 10 \mu\text{M}$) in living cells. The largely different redox potential between intracellular and extracellular compartments as well as the further elevated concentration of GSH in cancer cells promotes the disulfide-thiol degradation platform in the development of thiol-responsive degradable micellar nanocarriers for DDSs.^{42,43}

Several strategies to synthesis of thiol-responsive degradable ABPs and their nanosized assemblies have been reported.^{44–46}

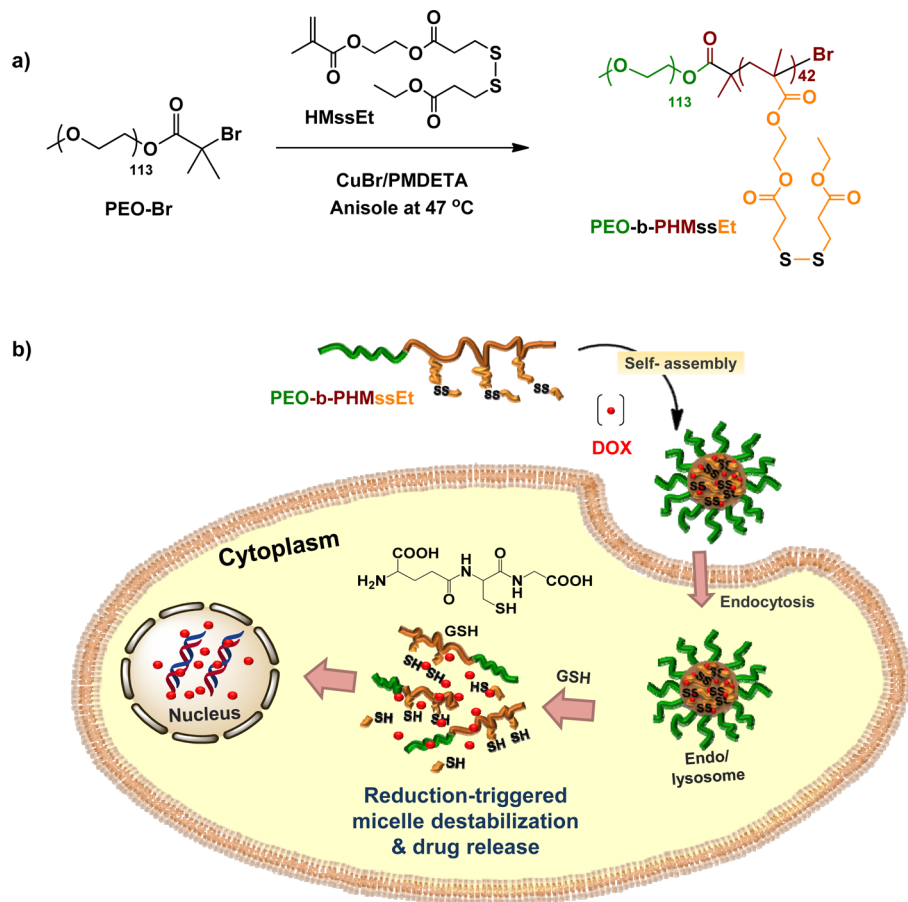
Received: April 5, 2013

Revised: May 2, 2013

Published: May 6, 2013



Scheme 1. (a) Preparation of Well-Controlled PEO-*b*-PHMssEt via ATRP and (b) Illustration of PEO-*b*-PHMssEt Micelles As Effective Intracellular Drug Delivery Nanocarriers Exhibiting Enhanced Release of DOX in Response to GSH in Cancer Cells



They are characterized with the different numbers or locations of disulfide linkages in micellar cores or at interfaces between cores and coronas. Typical examples include monocleavable micelles having single disulfide bonds in the middle of symmetric triblock copolymers,^{47–49} sheddable micelles having single disulfides at the junctions of diblock copolymers,^{50–52} and multicleavable micelles having disulfides positioned in hydrophobic main chains.^{53–62} These micelles exhibit the controlled release of encapsulated drugs through main chain degradation mechanism, causing the destabilization or disintegration of micellar aggregates. Another promising class of thiol-responsive degradable micelles consists of block copolymers having disulfide linkages as side chains (called pendant multicleavable micelles). The pendant disulfides in hydrophobic cores are cleaved in response to thiols, causing the dissociation of micelles due to the change in hydrophilic/hydrophobic balance.^{63–65} Alternatively, these micelles are converted to core-cross-linked micelles with disulfide cross-links through interchain thiol-disulfide polyexchange reactions in the presence reducing agents, providing enhanced colloidal stability and preventing premature release of encapsulated drugs during the circulation in the body. The newly formed disulfide cross-links are further cleaved in response to reductive reactions, causing the dissociation of micelles, thus enhancing the release of encapsulated drugs.^{66–70}

Recently, we have reported the synthesis of a new ABP consisting of a pendant disulfide-labeled polymethacrylate block (PHMssEt) and a hydrophilic poly(ethylene oxide) (PEO)

block by atom transfer radical polymerization (ATRP) of a new pendant disulfide-functionalized methacrylate (HMssEt) in the presence of PEO-Br macroinitiator (Scheme 1a).⁷¹ Its self-assembled nanostructures exhibited tunable release of encapsulated model drugs such as Nile Red (a hydrophobic fluorescent dye) in aqueous solutions with morphology changes, depending on the amount of added thiols such as D,L-dithiothreitol (DTT). In this paper, we have further evaluated thiol-responsive degradable PEO-*b*-PHMssEt micelles as effective intracellular drug delivery nanocarriers. In response to cellular GSH, the destabilization of these micelles due to change in pendant hydrophobic/hydrophilic balance upon cleavage of pendant disulfide linkages was followed by dynamic light scattering (DLS) technique; such micellar destabilization led to enhanced release of encapsulated doxorubicin (DOX) as a model anticancer drug. Further, GSH-responsive degradation of DOX-loaded micelles was investigated in cellular environments using flow cytometry and confocal laser scanning microscopy (CLSM) for cellular uptake as well as cell viability measurements. The results indicate that rapid DOX release from DOX-loaded micelles triggered by higher intracellular GSH concentration resulted in enhanced inhibition of the cellular proliferation after internalization (Scheme 1b).

EXPERIMENTAL SECTION

Materials. Copper(I) bromide (CuBr, >99.99%), *N,N,N',N'',N''-*pentamethyldiethylenetriamine (PMDETA, >98%), anisole, doxorubicin hydrochloride (DOX, $-\text{NH}_3^+\text{Cl}^-$ salt forms, >98%), triethylamine (Et_3N , > 99.5%), GSH (reduced form), and glutathione ethyl ester

(GSH-OEt, reduced form) were purchased from Aldrich and used as received. A water-soluble macroinitiator, poly(ethylene oxide) monomethyl ether (PEO)-functionalized bromoisobutyrate (PEO-Br, ethylene oxide units DP \approx 113),⁷² and a methacrylate bearing a pendant disulfide linkage (HMssEt)⁷¹ were synthesized using reported procedures.

Instrumentation. ¹H NMR spectra were recorded using a 500 MHz Varian spectrometer. The CDCl₃ singlet at 7.26 ppm was selected as the reference standard. Molecular weight and molecular weight distribution were determined by gel permeation chromatography (GPC). An Agilent GPC was equipped with a 1260 Infinity Isocratic Pump and a refractive index (RI) detector. Two Agilent columns (PLgel mixed-D and mixed-C) were used with dimethylformamide (DMF) containing 0.1 mol % LiBr at 50 °C at a flow rate of 1.0 mL/min. Linear poly(methyl methacrylate) (PMMA) standards from Fluka were used for calibration. Aliquots of polymer samples were dissolved in DMF/LiBr. The clear solutions were filtered using a 0.25 μm PTFE filter to remove any DMF-insoluble species. A drop of anisole was added as a flow rate marker. The size of micelles in hydrodynamic diameter by volume was measured by DLS at a fixed scattering angle of 175° at 25 °C with a Malvern Instruments Nano S ZEN1600 equipped with a 633 nm He–Ne gas laser. UV/vis spectra were recorded on Agilent Cary 60 UV/vis spectrometer.

Synthesis of PEO-*b*-PHMssEt Using ATRP. The detailed procedure for the synthesis of PEO-*b*-PHMssEt is described in our previous report.⁷¹ Briefly, a mixture consisting of PEO-Br (0.3 g, 0.06 mmol), HMssEt (1.2 g, 3.4 mmol), PMDETA (4.5 mg, 0.03 mmol), CuBr (2.9 mg, 0.02 mmol), and anisole (4.0 mL) in a 25 mL Schlenk flask was immersed in an oil bath preheated at 50 °C to start polymerization. After 4 h, polymerization was stopped by cooling and exposing the reaction mixture to air. The resulting polymers were purified as follows; the as-synthesized polymer solution was passed through a basic alumina column to remove the copper complex, and then solvents were removed by rotary evaporation. The products were precipitated from hexane three times, and then dried in vacuum oven at room temperature for 18 h. Molecular weight by GPC: M_n = 25 400 g/mol with M_w/M_n = 1.1.

Aqueous Micellization of PEO-*b*-PHMssEt Using a Dialysis Method. Water (9 mL) was added dropwise to a clear solution of PEO-*b*-PHMssEt (10 mg) dissolved in DMF (2 mL). The resulting mixture was stirred for 2 h, and then dialyzed in a dialysis tubing (MWCO = 12 000 g/mol) against water for 3 days to remove DMF. The outer water (500 mL) was changed twice a day, yielding colloidally stable micellar aggregates in aqueous solution at 1 mg/mL concentration.

Preparation of DOX-Loaded Micelles. Similar procedure for aqueous micellization through the dialysis method was used. For the preparation of the sample of MDOX-1, water (5 mL) was added dropwise to the solution consisting of the purified, dried PEO-*b*-PHMssEt (20 mg), DOX (1 mg), and Et₃N (3 mol equiv to DOX) in DMF (2 mL). The resulting dispersion was dialyzed over water (500 mL) for 5 days, yielding a DOX-loaded micellar dispersion at 2.6 mg/mL concentration. For the MDOX-2 at 1.7 mg/mL, a similar procedure was used except for the use of increasing amounts of PEO-*b*-PHMssEt (20 mg), DOX (2 mg), DMF (3 mL), and water (10 mL).

Determination of Loading Level of DOX Using UV/Vis Spectroscopy. A calibration curve of absorbance (A) at $\lambda_{\text{max}} = 480$ nm over various concentrations of DOX in DMF was first constructed as follows. A stock solution of DOX in DMF (1 mg/mL, 1.7 mmol/L) was prepared by dissolving DOX (1 mg, 1.7 μmol) in DMF (1 mL). Aliquots of the stock solution were then diluted with DMF to form a series of solutions of DOX with different concentrations ranging from 5.6 to 19.5 μmol/L. Their UV/vis spectra ($\lambda_{\text{ex}} = 480$ nm) were recorded. Next, the loading level of DOX for DOX-loaded micelles was determined as follows: aliquots of DOX-loaded micellar dispersion (1 mL) were taken. After the removal of water using a rotary evaporation, the residues of DOX and copolymers were dissolved in DMF (2 mL) to form clear solutions. Their UV/vis spectra were recorded and the loading level of DOX was calculated by the weight ratio of loaded DOX to dried polymers.

Reductive Cleavage of Disulfide Linkages of PEO-*b*-PHMssEt in DMF. An aliquot of dried, purified PEO-*b*-PHMssEt (20 mg) was mixed with DTT (33 mg, 0.22 mmol, Acros Organics) in DMF (2.0 mL) under stirring at room temperature. After 30 min, aliquots were taken to analyze molecular weight distribution of degraded products using GPC.

GSH-Triggered Destabilization of Aqueous PEO-*b*-PHMssEt Micelles. Aliquots of aqueous micellar dispersion (1 mg/mL, 10 mL) were mixed with GSH (30 mg, 97 μmol, 10 mM) under stirring. An aliquot was taken to analyze their size distributions using DLS.

GSH-Triggered Release of DOX from Aqueous DOX-Loaded Micelles. Aliquots of DOX-loaded micellar dispersion (MDOX-2, 1.7 mg/mL, 10 mL) were transferred into a dialysis tubing (MWCO = 12 000 g/mol) and immersed in aqueous KH₂PO₄ buffer solution (100 mL, pH = 7.0) as a control and 10 mM aqueous GSH solution buffered with KH₂PO₄ at pH = 7.0 under stirring. The absorbance of DOX in outer water was recorded at an interval of 8 min using a UV/vis spectrometer equipped with an external probe at $\lambda_{\text{ex}} = 497$ nm. For quantitative analysis, DOX (122.4 μg, equivalent to DOX encapsulated in 10 mL MDOX-2) was dissolved in 10 mM aqueous GSH solution buffered with KH₂PO₄ (pH = 7.0), and its UV/vis spectrum was recorded.

Cell Culture. Human embryonic kidney (HEK293T) and HeLa cancer cells were cultured in Dulbecco's modified Eagle's medium (DMEM) containing 10% fetal bovine serum (FBS) and 1% antibiotics (50 units/mL penicillin and 50 units/mL streptomycin) at 37 °C in a humidified atmosphere containing 5% CO₂.

Flow Cytometry. Cells plated at 5×10^5 cells/well into a six-well plate and incubated for 24 h in DMEM (2 mL) were treated with and without GSH-OEt (10 mM in cell medium) for 12 h. Cells were washed with phosphate-buffered saline (PBS) buffer, and then incubated with DOX-loaded micelles (200 μL for DOX = 1.9 μg/mL) at 37 °C for 1 h. After culture medium was removed, cells were washed with PBS buffer three times and then treated with trypsin. The cells were suspended in DMEM (300 μL) for flow cytometry measurements. Data analysis was performed by means of a BD FACSCANTO II flow cytometer and BD FACSDiva software.

CLSM. HeLa cells plated at 2×10^5 cells/well into a 24-well plate and incubated for 24 h in DMEM (100 μL) were treated with and without GSH-OEt (10 mM in cell medium) for 12 h. Cells were washed with PBS buffer, and then incubated with DOX-loaded micelles (DOX = 5.1 μg/mL) at 37 °C for 24 h. After culture medium was removed, cells were washed with PBS buffer three times. After the removal of supernatants, the cells were fixed with cold methanol (−20 °C) for 20 min at 4 °C. The slides were rinsed with TBST (tris-buffered saline Tween-20) for three times. Cells were stained with 2-(4-amidinophenyl)-6-indolecarbamidine (DAPI) for 5 min. The fluorescence images were obtained using a LSM 510 Meta/Axiovert 200 (Carl Zeiss, Jena, Germany).

Cell Viability Using MTT Assay. HEK293T and HeLa cells were plated at 5×10^5 cells/well into a 96-well plate and incubated for 24 h in DMEM (100 μL) containing 10% FBS. They were then incubated with various concentrations of micellar dispersions of PEO-*b*-PHMssEt for 48 h. Blank controls without micelles (cells only) were run simultaneously. Cell viability was measured using CellTiter 96 Non-Radioactive Cell Proliferation Assay kit (MTT, Promega) according to manufacturer's instruction. Briefly, 3-(4,5-dimethylthiazol-2-yl)-2,5-diphenyltetrazolium bromide (MTT) solutions (15 μL) was added into each well. After 4 h incubation, the medium containing unreacted MTT was carefully removed. Dimethyl sulfoxide (DMSO; 100 μL) was added into each well in order to dissolve the formed formazan blue crystals, and then the absorbance at $\lambda = 570$ nm was recorded using Powerwave HT Microplate Reader (Bio-Tek). Each concentration was 12-replicated. Cell viability was calculated as the percent ratio of absorbance of mixtures with micelles to control (cells only).

Intracellular DOX Release and HeLa Cell Viability. HeLa cells were plated at 5×10^5 cells/well into a 96-well plate and incubated for 24 h in DMEM (100 μL). They were then treated with and without GSH-OEt (10 mM in cell medium) for 12 h, and then incubated with

different amounts of DOX-loaded micellar dispersion (MDOX-1, 2.8 mg/mL) for 48 h. Blank controls without micelles (cells only) were run simultaneously to calculate viability as described above.

RESULTS AND DISCUSSION

Synthesis and Aqueous Micellization of PEO-*b*-PHMssEt. Well-controlled PEO-*b*-PHMssEt block copolymer was synthesized by ATRP,^{73,74} a well-established controlled radical polymerization (CRP) method.⁷⁵ The ATRP enables the synthesis of well-defined copolymers with predetermined molecular weight, narrow molecular weight distributions, and various functionalities and architectures. In our experiments, PEO-Br was synthesized and used as a hydrophilic macroinitiator for the ATRP of HMssEt mediated with CuBr/PMDETA active complex in anisole at 47 °C for 4 h. The resulting polymers were purified by the removal of unreacted HMssEt monomers and Cu species. They were characterized with the degree of polymerization of PHMssEt block (DP) = 42 by ¹H NMR, as well as the number average molecular weight $M_n = 25,400$ g/mol with molecular weight distribution $M_w/M_n = 1.1$ by GPC (Figure 1). These results suggest the synthesis of well-controlled PEO₁₁₃-*b*-PHMssEt₄₂ with narrow molecular weight distribution having 42 pendant disulfide linkages per each polymer chain.

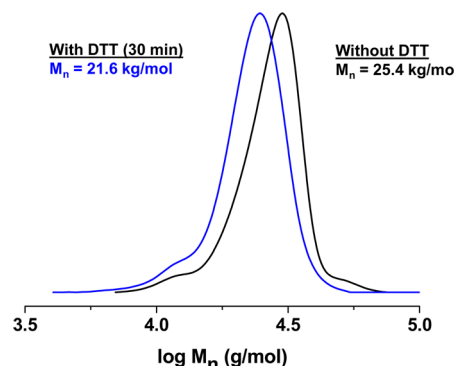


Figure 1. GPC traces of PEO-*b*-PHMssEt before and 30 min after treatment with DTT (5 mol equivalents to disulfide linkages) in DMF.

The resulting PEO-*b*-PHMssEt is amphiphilic and self-assemble to form micellar aggregates in an aqueous solution. Its critical micellar concentration (CMC) was determined to be 49 µg/mL using tensiometry. Aqueous micellization using a solvent evaporation method with tetrahydrofuran (THF) resulted in the formation of colloidally stable spherical micellar aggregates with a diameter of 50.9 ± 0.5 nm by DLS and 40.1 ± 6.7 nm by TEM at 1.0 mg/mL concentration.⁷¹ Here,

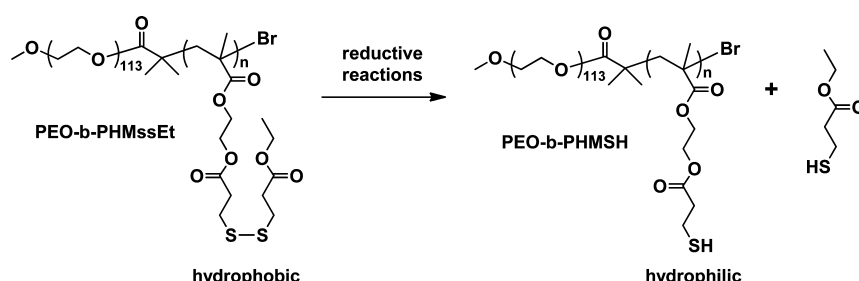
aqueous micellization through a dialysis method was examined to prepare micellar aggregates at 0.9 mg/mL concentration. DLS results indicate their number average diameter (D_n) to be 145.2 ± 0.7 nm with relatively narrow size distribution (polydispersity, $D_w/D_n < 1.15$) (Figure S1, Supporting Information). Interestingly, the size of micelles prepared by dialysis method is larger than that prepared by the solvent evaporation method.

Destabilization of Micellar Aggregates in Response to GSH. The micellar aggregates prepared by aqueous micellization through self-assembly contain pendant disulfide linkages in hydrophobic cores. As seen in Scheme 2, the disulfide linkages in PHMssEt blocks are cleaved in response to reducing agents such as DTT and cellular GSH to the corresponding thiols (PHMSH). Such cleavage of pendant disulfide linkages is evidenced with a decrease in molecular weight from $M_n = 25.4$ kg/mol to $M_n = 21.7$ kg/mol when PEO-*b*-PHMssEt was treated with DTT in DMF (Figure 1).

For aqueous micellar aggregates, thiol-responsive cleavage results in the change in hydrophobic/hydrophilic balance, leading to the destabilization of micelles. However, DTT is not a cellular component and is smaller than GSH in size; thus, it will be expected that DTT will gain access to disulfides in micellar cores faster than GSH. Here, we investigated the response of PHMssEt blocks in micellar cores to water-soluble GSH in aqueous solution. DLS technique was used to follow the change in size distribution of aqueous micellar aggregates in the absence and presence of 10 mM GSH (Figure 2). In the absence of GSH as a control, no significant change in size distribution occurred over 20 h. In the presence of 10 mM GSH, however, the size distribution became bimodal with the occurrence of large aggregates (diameter >1 µm) in 2 h. Further, the distribution became broader as the population of the large aggregates increased over 20 h. Such size change was also followed by the increase in z-average diameter of micelles over time (Figure S2). These results suggest that micellar aggregates are destabilized due to the degradation of PHMssEt micellar cores upon the cleavage of disulfide linkages in response to water-soluble GSH. Similar increase in micellar size is reported for other degradable micelles having pendant disulfides⁶¹ or acid-labile linkages.^{76,77}

Loading and GSH-Triggered Release of DOX from DOX-Loaded Micelles. DOX (called adriamycin or hydroxydaunorubicin) is a DNA-interacting anticancer drug used in chemotherapy. Here, DOX was encapsulated in hydrophobic micellar cores using the dialysis method for the dispersed mixtures consisting of PEO-*b*-PHMssEt, DOX ($-\text{NH}_2$ forms) converted by treatment of DOX ($-\text{NH}_3^+\text{Cl}^-$ salt forms) with Et₃N (a base), DMF, and water. Free DOX and DMF were

Scheme 2. Reductive Cleavage of Pendant Disulfide Linkages of PEO-*b*-PHMssEt to the Corresponding PEO-*b*-PHMSH Hydrophilic Block Copolymers



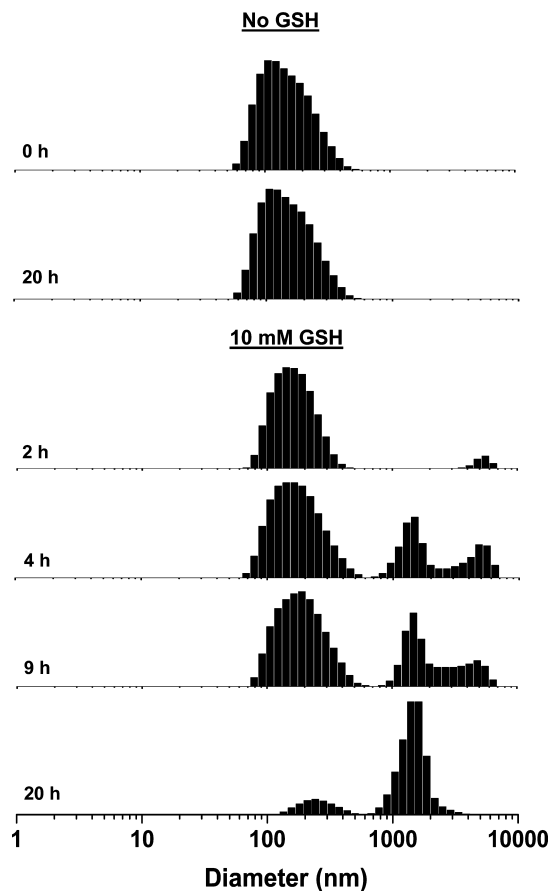


Figure 2. Evolution of DLS diagrams (volume %) of PEO-*b*-PHMssEt micellar aggregates in aqueous buffer solution as control and in 10 mM aqueous GSH buffer solution over time.

then removed by intensive dialysis using a dialysis tubing (molecular weight cutoff (MWCO) = 12 000 g/mol) for over 5 days. The removal of free DOX was monitored by measuring the absorbance of DOX at 497 nm in outer water (Figure S3). The size and morphology of aqueous DOX-loaded micellar aggregates were then examined using DLS and transmission electron microscopy (TEM) at a micellar concentration of 2.6 mg/mL. DLS results suggest the presence of two populations with *z*-average diameter based on light scattering intensity to be 174 ± 19 nm. The main population (>95% volume) is smaller-sized aggregates having $D_n = 190 \pm 32$ nm with relatively broad size distribution ($D_w/D_n > 1.33$), while a smaller population (<5% volume) is larger-sized aggregates with the diameter >1 μm (Figure 3a). TEM images also indicate broad distribution of spherical micelles with average diameter = 81.3 ± 25.9 nm (Figure 3b). The smaller micellar size determined by TEM than by DLS is attributed to the dehydrated state of the micelles.⁷⁸

The loading level of DOX for DOX-loaded micelles was determined using UV/vis spectroscopy. As seen in Figure S4, a calibration curve of absorbance at $\lambda_{\text{max}} = 480$ nm over the concentrations of DOX in DMF was first constructed, and its extinction coefficient (ϵ) was determined to be $11\,700\text{ M}^{-1}\text{ cm}^{-1}$. Next, for DOX-loaded micellar dispersions prepared as above, water was removed by rotary evaporation, and the residues were dissolved in DMF to form clear solutions of DOX and PEO-*b*-PHMssEt. Figure 4 shows a typical UV/vis spectrum of DOX-loaded micelles in DMF, which is similar to that of free DOX in DMF, suggesting no significant change in

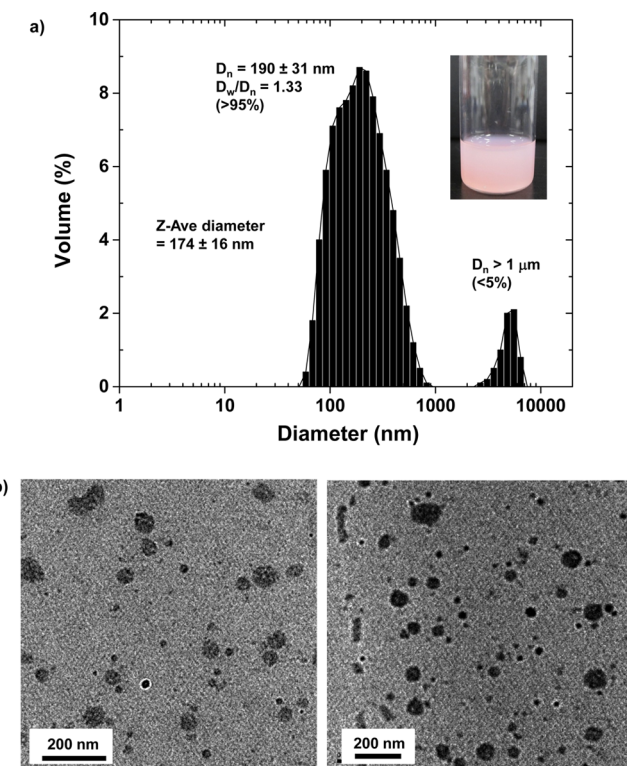


Figure 3. DLS diagram (a) and TEM images (b) of DOX-loaded micelles of PEO-*b*-PHMssEt at 2.5 mg/mL concentration prepared by dialysis method (inset of (a): digital picture of DOX-loaded micellar dispersion).

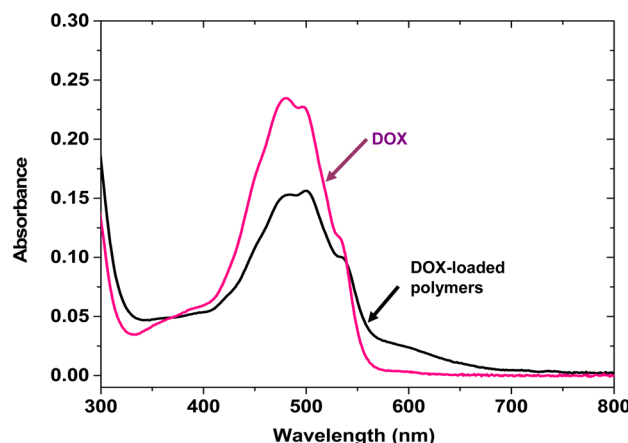


Figure 4. A typical UV/vis spectrum of DOX-loaded micelles after the removal of water, compared with that of free DOX (19.5 $\mu\text{mol}/\text{mL}$) in DMF.

the structure of DOX encapsulated in hydrophobic micellar cores. Using the Beer–Lambert equation with the absorbance at $\lambda_{\text{max}} = 480$ nm and the extinction coefficient, the loading level of DOX was determined to be $0.44 \pm 0.07\%$ for MDOX-1 and $0.81 \pm 0.07\%$ for MDOX-2 (Table 1). Similarly, the DOX loading level increased when the initial amount of DOX mixed with polymer in the feed increased.⁷⁹

Next, the release of DOX from DOX-loaded micelles upon redox-cleavage of pendant disulfide linkages in the micellar core was investigated. An aliquot of DOX-loaded micellar dispersion in dialysis tubing was placed in 10 mM aqueous GSH solution buffered with KH_2PO_4 at $\text{pH} = 7$ and aqueous buffer solution

Table 1. Loading Level of DOX for DOX-Loaded PEO-*b*-PHMssEt Micelles Prepared by the Dialysis Method over 5 Days

| sample | DOX/polymer (mg/mg) | water/polymer (mL/mg) | DOX-loaded micelles (mg/mL) | loading (%) |
|--------|---------------------|-----------------------|-----------------------------|-------------|
| MDOX-1 | 1/20 | 5/20 | 2.8 | 0.44 ± 0.07 |
| MDOX-2 | 2/20 | 10/20 | 1.7 | 0.81 ± 0.07 |

(pH = 7) as a control. Figure 5 shows % DOX released from DOX-loaded micelles in the absence and presence of 10 mM

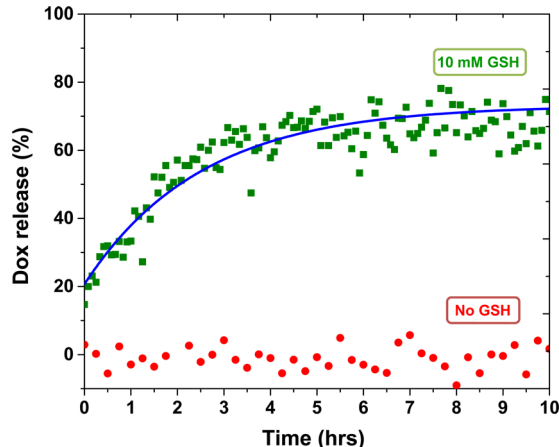


Figure 5. Release of DOX from DOX-loaded micelles in 10 mM aqueous GSH solution buffered with KH₂PO₄ at pH = 7.0, and aqueous KH₂PO₄ buffer solution at pH = 7.0 as a control.

GSH. In the absence of GSH, no significant release of DOX was observed because DOX is presumably confined in small micellar cores. In the presence of 10 mM GSH, however, DOX-loaded micelles degrade to the corresponding water-soluble PEO-*b*-PHMSH, causing the enhanced release of encapsulated DOX to aqueous solution. >70% DOX was released from the micelles within 5 h.

GSH-Responsive Intracellular Release of DOX upon Degradation. Cellular uptake and intracellular release of DOX in response to cellular GSH for HeLa cancer cells were investigated using flow cytometry and CLSM. In biological systems, cellular GSH-OEt can penetrate cellular membranes and rapidly reach a high intracellular concentration of GSH.⁸⁰ In our experiments, HeLa cells were pretreated with and without 10 mM aqueous GSH-OEt solution for 12 h to manipulate the intracellular concentration of GSH. Several reports also describe the pretreatment of cancer cells with GSH-OEt to enhance cellular GSH levels.^{51,53,57} Figure 6 shows flow cytometric histograms of HeLa cells. Compared to cells only as controls, the histograms for HeLa cells incubated with DOX-loaded micelles were shifted clearly to the direction of high fluorescence intensity, suggesting internalization of DOX-loaded micelles in HeLa cells. More importantly, HeLa cells pretreated with 10 mM GSH-OEt had higher fluorescence intensity than cells not pretreated with GSH-OEt, as results from degradation of pendant disulfide linkages in response to GSH, accelerating intracellular release of DOX from the micelles. Intracellular release of DOX was further investigated using CLSM. Figure 7 shows CLSM images of HeLa cells incubated with DOX-loaded micelles for 24 h. HeLa nuclei were stained with DAPI. For both cells being pretreated

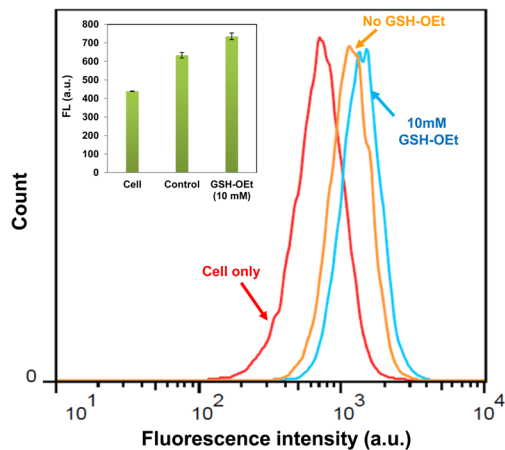


Figure 6. Flow cytometric histograms of HeLa cells pretreated with and without 10 mM GSH-OEt and then incubated with DOX-loaded PEO-*b*-PHMssEt micelles for 2 h.

without and with 10 mM GSH-OEt, the images from DOX fluorescence suggest that DOX-loaded micelles were internalized, and DOX was released to reach cell nuclei. Importantly, DOX fluorescence was brighter when HeLa was pretreated with 10 mM GSH-OEt, compared to cells not pretreated with GSH-OEt (Figure 7b).

In Vitro Cytotoxicity of DOX-Loaded Micelles. MTT colorimetric assay was used to evaluate the cytotoxicity of DOX-free (or blank) and DOX-loaded micelles of PEO-*b*-PHMssEt. First, blank micelles exhibited >80% viability of both HEK293T healthy kidney cells and HeLa cancer cells after 48 h incubation at the micellar concentration up to 510 µg/mL. These results suggest nontoxicity of PEO-*b*-PHMssEt to different cell lines (Figure 8). Next, the cytotoxicity of DOX-loaded micelles upon their GSH-responsive degradation was examined. Here, HeLa cells were also pretreated with and without 10 mM aqueous GSH-OEt solution for 12 h and then incubated with various amounts of DOX-loaded micelles for 48 h. Cells were also incubated with free DOX for comparison. As seen in Figure 9, the viability of HeLa cells decreased with an increasing amount of both free and encapsulated DOX, suggesting inhibition of cell proliferation in the presence of DOX. In the presence of DOX-loaded micelles, however, the viability is lower when HeLa cells were pretreated with GSH-OEt, compared to no GSH-OEt pretreatment. Note that 10 mM GSH-OEt is not cytotoxic to HeLa cells in our experiment (Figure S6) and others.^{50,81} Thus, the lower viability of HeLa cells pretreated with GSH-OEt is attributed to the presence of more GSH in HeLa cells that causes the enhanced release of DOX upon cleavage of disulfide linkages to inhibit the proliferation of HeLa cells. The viability in the presence of DOX-loaded micelles with no GSH-OEt treatment was slightly lower, compared to blank micelles; this could be due to the presence of GSH found in HeLa cancer cells that can trigger the degradation of DOX-loaded micelles.

The results from flow cytometry, CLSM, and cell viability measurements suggest faster DOX release from DOX-loaded micelles triggered by higher intracellular GSH concentration, enhancing the inhibition of the cellular proliferation after internalization.

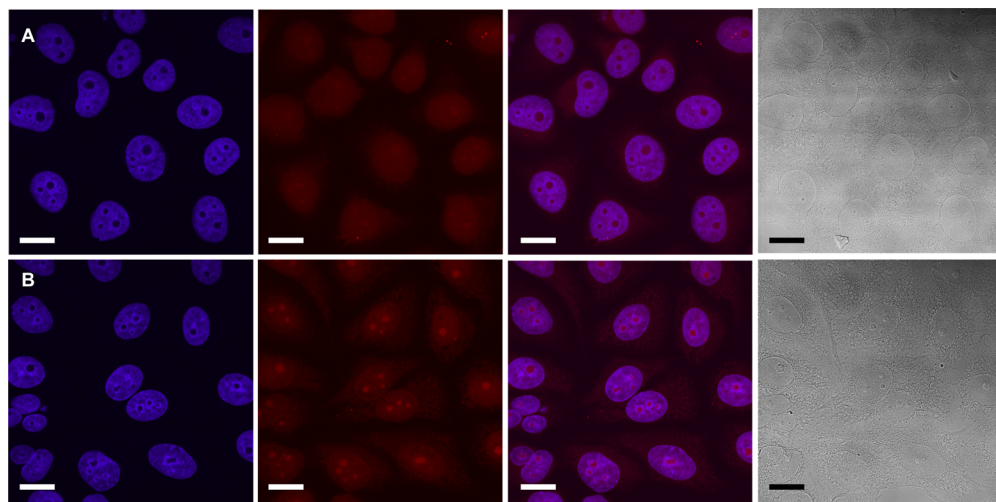


Figure 7. CLSM images of HeLa cells pretreated without (A) and with (B) 10 mM GSH-OEt and then incubated with DOX-loaded PEO-*b*-PHMssEt micelles for 24 h. For each panel, the images from left to right show cell nuclei stained by DAPI (blue), DOX fluorescence in cells (red), overlays of two images, and differential interference contrast (DIC) image. Scale bar = 20 μ m.

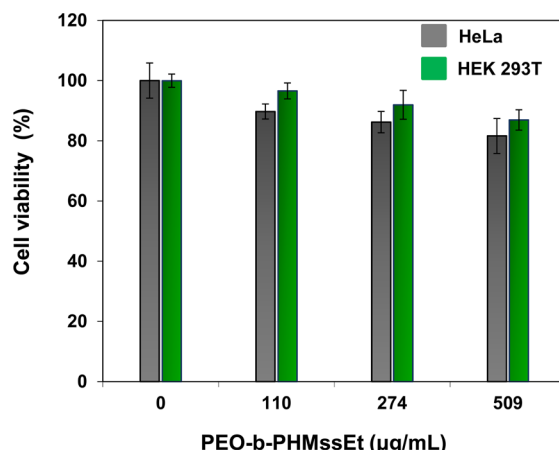


Figure 8. Viability of HeLa and HEK 293T cells incubated with different amounts of PEO-*b*-PHMssEt micelles for 48 h determined by MTT assay. Data are presented as the average \pm standard deviation ($n = 12$).

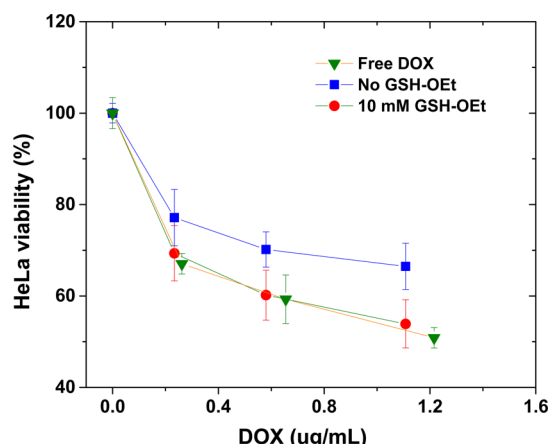


Figure 9. Viability of HeLa cells pretreated with and without 10 mM GSH-OEt and then incubated with different amounts of free DOX and DOX-loaded micelles for 48 h. Data are presented as average \pm standard deviation ($n = 12$).

CONCLUSION

Well-controlled PEO-*b*-PHMssEt ABPs having pendant disulfide linkages synthesized by ATRP self-assembled to form colloidally stable micellar aggregates in aqueous solutions above the CMC. They exhibited reduction-responsive degradation properties; consequently, pendant disulfide linkages in micellar cores were cleaved in the presence of GSH, resulting in degradation or destabilization of micellar nanocarriers. Such degradation led to the enhanced release of encapsulated anticancer drugs in aqueous solutions, which was followed by DLS and UV absorbance measurements, as well as in cellular environments, which was analyzed using MTT-based cell viability measurements. Intracellular release of anticancer drugs after internalization into HeLa cancer cells was evidenced by flow cytometry and CLSM. These significant results suggest that GSH-responsive PEO-*b*-PHMssEt micelles hold great promise as intracellular nanocarriers exhibiting the enhanced release of encapsulated anticancer drugs through biodegradation in response to cellular GSH.

ASSOCIATED CONTENT

Supporting Information

Additional characterization plots. This material is available free of charge via the Internet at <http://pubs.acs.org>.

AUTHOR INFORMATION

Corresponding Author

*E-mail: john.oh@concordia.ca.

Notes

The authors declare no competing financial interest.

ACKNOWLEDGMENTS

This work is supported by an NSERC Discovery Grant and Canada Research Chair (CRC) Award. The authors thank Dr. Qian Zhang and Samuel Aleksanian for the synthesis of PEO-*b*-PHMssEt and PEO-Br polymer, as well as Prof. Alisa Pieckny and Tara Akhshi for helpful discussions. J.K.O. is entitled Tier II CRC in Nanobioscience as well as a member of Centre Québécois sur les Matériaux Fonctionnels (CQMF) funded by FQRNT.

■ REFERENCES

- (1) Langer, R.; Tirrell, D. A. *Nature* **2004**, *428*, 487–492.
- (2) Langer, R. *Acc. Chem. Res.* **2000**, *33*, 94–101.
- (3) Hoffman, A. S.; Stayton, P. S.; Press, O.; Murthy, N.; Lackey, C. A.; Cheung, C.; Black, F.; Campbell, J.; Fausto, N.; Kyriakides, T. R.; Bornstein, P. *Polym. Adv. Technol.* **2002**, *13*, 992–999.
- (4) Hoffman, A. S. *Adv. Drug Delivery Rev.* **2002**, *54*, 3–12.
- (5) Peppas, N. A. *Adv. Drug Delivery Rev.* **2004**, *56*, 1529–1531.
- (6) Harada, A.; Kataoka, K. *Prog. Polym. Sci.* **2006**, *31*, 949–982.
- (7) Mikhail, A. S.; Allen, C. J. *Controlled Release* **2009**, *138*, 214–223.
- (8) Xiong, X.-B.; Falamarzian, A.; Garg, S. M.; Lavasanifar, A. J. *Controlled Release* **2011**, *155*, 248–261.
- (9) Klinger, D.; Landfester, K. *Polymer* **2012**, *53*, 5209–5231.
- (10) Wang, Y.; Xu, H.; Zhang, X. *Adv. Mater.* **2009**, *21*, 2849–2864.
- (11) Jackson, A. W.; Fulton, D. A. *Polym. Chem.* **2013**, *4*, 31–45.
- (12) Zhang, Q.; Ko, N. R.; Oh, J. K. *Chem. Commun.* **2012**, *48*, 7542–7552.
- (13) Cayre, O. J.; Chagneux, N.; Biggs, S. *Soft Matter* **2011**, *7*, 2211–2234.
- (14) Loomis, K.; McNeeley, K.; Bellamkonda, R. V. *Soft Matter* **2011**, *7*, 839–856.
- (15) Rijcken, C. J. F.; Soga, O.; Hennink, W. E.; van Nostrum, C. F. J. *Controlled Release* **2007**, *120*, 131–148.
- (16) Zhang, Q.; Noh, S. M.; Nam, J. H.; Jung, H. W.; Park, J. M.; Oh, J. K. *Macromol. Rapid Commun.* **2012**, *33*, 1528–1534.
- (17) Phillips, D. J.; Gibson, M. I. *Chem. Commun.* **2012**, *48*, 1054–1056.
- (18) Monge, S.; Antoniacomi, S.; Lapinte, V.; Darcos, V.; Robin, J.-J. *Polym. Chem.* **2012**, *3*, 2502–2507.
- (19) Zhang, L.-J.; Dong, B.-T.; Du, F.-S.; Li, Z.-C. *Macromolecules* **2012**, *45*, 8580–8587.
- (20) Dong, W.-F.; Kishimura, A.; Anraku, Y.; Chuano, S.; Kataoka, K. *J. Am. Chem. Soc.* **2009**, *131*, 3804–3805.
- (21) Ku, T.-H.; Chien, M.-P.; Thompson, M. P.; Sinkovits, R. S.; Olson, N. H.; Baker, T. S.; Gianneschi, N. C. *J. Am. Chem. Soc.* **2011**, *133*, 8392–8395.
- (22) Khorsand Sourkohi, B.; Schmidt, R.; Oh, J. K. *Macromol. Rapid Commun.* **2011**, *32*, 1652–1657.
- (23) Zhang, M.; Yang, L.; Yurt, S.; Misner, M. J.; Chen, J.-T.; Coughlin, E. B.; Venkataraman, D.; Russell, T. P. *Adv. Mater.* **2007**, *19*, 1571–1576.
- (24) Zhao, H.; Gu, W.; Sterner, E.; Russell, T. P.; Coughlin, E. B.; Theato, P. *Macromolecules* **2011**, *44*, 6433–6440.
- (25) Kang, M.; Moon, B. *Macromolecules* **2009**, *42*, 455–458.
- (26) Ma, N.; Li, Y.; Xu, H.; Wang, Z.; Zhang, X. *J. Am. Chem. Soc.* **2010**, *132*, 442–443.
- (27) Du, J.-Z.; Chen, D.-P.; Wang, Y.-C.; Xiao, C.-S.; Lu, Y.-J.; Wang, J.; Zhang, G.-Z. *Biomacromolecules* **2006**, *7*, 1898–1903.
- (28) Gillies, E. R.; Frechet, J. M. J. *Chem. Commun.* **2003**, 1640–1641.
- (29) Huang, X.-N.; Du, F.-S.; Zhang, B.; Zhao, J.-Y.; Li, Z.-C. *J. Polym. Sci., Part A: Polym. Chem.* **2008**, *46*, 4332–4343.
- (30) Jin, Y.; Song, L.; Su, Y.; Zhu, L.; Pang, Y.; Qiu, F.; Tong, G.; Yan, D.; Zhu, B.; Zhu, X. *Biomacromolecules* **2011**, *12*, 3460–3468.
- (31) Binauld, S.; Stenzel, M. H. *Chem. Commun.* **2013**, *49*, 2082–2102.
- (32) Brinkhuis, R. P.; Visser, T. R.; Rutjes, F. P. J. T.; van Hest, J. C. M. *Polym. Chem.* **2011**, *2*, 550–552.
- (33) Zhao, Y. *Macromolecules* **2012**, *45*, 3647–3657.
- (34) Zhao, H.; Sterner, E. S.; Coughlin, E. B.; Theato, P. *Macromolecules* **2012**, *45*, 1723–1736.
- (35) Schumers, J.-M.; Fustin, C.-A.; Gohy, J.-F. *Macromol. Rapid Commun.* **2010**, *31*, 1588–1607.
- (36) Wang, J.; Pelletier, M.; Zhang, H.; Xia, H.; Zhao, Y. *Langmuir* **2009**, *25*, 13201–13205.
- (37) Geers, B.; Dewitte, H.; De Smedt, S. C.; Lentacker, I. J. *Controlled Release* **2012**, *164*, 248–255.
- (38) Kim, H.; Kang, Y. J.; Kang, S.; Kim, K. T. *J. Am. Chem. Soc.* **2012**, *134*, 4030–4033.
- (39) Yao, Y.; Zhao, L.; Yang, J.; Yang, J. *Biomacromolecules* **2012**, *13*, 1837–1844.
- (40) Li, C.; Madsen, J.; Armes, S. P.; Lewis, A. L. *Angew. Chem., Int. Ed.* **2006**, *45*, 3510–3513.
- (41) Tsarevsky, N. V.; Matyjaszewski, K. *Macromolecules* **2005**, *38*, 3087–3092.
- (42) Russo, A.; DeGraff, W.; Friedman, N.; Mitchell, J. B. *Cancer Res.* **1986**, *46*, 2845–2848.
- (43) Saito, G.; Swanson, J. A.; Lee, K.-D. *Adv. Drug Delivery Rev.* **2003**, *55*, 199–215.
- (44) Meng, F.; Hennink, W. E.; Zhong, Z. *Biomaterials* **2009**, *30*, 2180–2198.
- (45) Cheng, R.; Feng, F.; Meng, F.; Deng, C.; Feijen, J.; Zhong, Z. *J. Controlled Release* **2011**, *152*, 2–12.
- (46) Wei, H.; Zhuo, R.-X.; Zhang, X.-Z. *Prog. Polym. Sci.* **2013**, *38*, 503–535.
- (47) Sun, L.; Liu, W.; Dong, C.-M. *Chem. Commun.* **2011**, *47*, 11282–11284.
- (48) Cunningham, A.; Oh, J. K. *Macromol. Rapid Commun.* **2013**, *34*, 163–168.
- (49) Li, S.; Ye, C.; Zhao, G.; Zhang, M.; Zhao, Y. *J. Polym. Sci., Part A: Polym. Chem.* **2012**, *50*, 3135–3148.
- (50) Liu, J.; Pang, Y.; Huang, W.; Huang, X.; Meng, L.; Zhu, X.; Zhou, Y.; Yan, D. *Biomacromolecules* **2011**, *12*, 1567–1577.
- (51) Tang, L.-Y.; Wang, Y.-C.; Li, Y.; Du, J.-Z.; Wang, J. *Bioconjugate Chem.* **2009**, *20*, 1095–1099.
- (52) Klaikherd, A.; Nagamani, C.; Thayumanavan, S. *J. Am. Chem. Soc.* **2009**, *131*, 4830–4838.
- (53) Wen, H.-Y.; Dong, H.-Q.; Xie, W.-j.; Li, Y.-Y.; Wang, K.; Pauletti, G. M.; Shi, D.-L. *Chem. Commun.* **2011**, *47*, 3550–3552.
- (54) Sun, H.; Guo, B.; Li, X.; Cheng, R.; Meng, F.; Liu, H.; Zhong, Z. *Biomacromolecules* **2010**, *11*, 848–854.
- (55) Khorsand Sourkohi, B.; Cunningham, A.; Zhang, Q.; Oh, J. K. *Biomacromolecules* **2011**, *12*, 3819–3825.
- (56) Zhang, Q.; Ko, N. R.; Oh, J. K. *RSC Adv.* **2012**, *2*, 8079–8086.
- (57) Liu, J.; Pang, Y.; Huang, W.; Zhu, Z.; Zhu, X.; Zhou, Y.; Yan, D. *Biomacromolecules* **2011**, *12*, 2407–2415.
- (58) Han, D.; Tong, X.; Zhao, Y. *Langmuir* **2012**, *28*, 2327–2331.
- (59) Nelson-Mendez, A.; Aleksanian, S.; Oh, M.; Lim, H.-S.; Oh, J. K. *Soft Matter* **2011**, *7*, 7441–7452.
- (60) Aleksanian, S.; Khorsand, B.; Schmidt, R.; Oh, J. K. *Polym. Chem.* **2012**, *3*, 2138–2147.
- (61) Fan, H.; Huang, J.; Li, Y.; Yu, J.; Chen, J. *Polymer* **2010**, *51*, 5107–5114.
- (62) Tong, R.; Xia, H.; Lu, X. *J. Mater. Chem. B* **2013**, *1*, 886–894.
- (63) Ryu, J.-H.; Roy, R.; Ventura, J.; Thayumanavan, S. *Langmuir* **2010**, *26*, 7086–7092.
- (64) Yuan, L.; Liu, J.; Wen, J.; Zhao, H. *Langmuir* **2012**, *28*, 11232–11240.
- (65) Chen, W.; Zou, Y.; Jia, J.; Meng, F.; Cheng, R.; Deng, C.; Feijen, J.; Zhong, Z. *Macromolecules* **2013**, *46*, 699–707.
- (66) Dai, J.; Lin, S.; Cheng, D.; Zou, S.; Shuai, X. *Angew. Chem., Int. Ed.* **2011**, *50*, 9404–9408.
- (67) Yan, L.; Wu, W.; Zhao, W.; Qi, R.; Cui, D.; Xie, Z.; Huang, Y.; Tong, T.; Jing, X. *Polym. Chem.* **2012**, *3*, 2403–2412.
- (68) Wei, R.; Cheng, L.; Zheng, M.; Cheng, R.; Meng, F.; Deng, C.; Zhong, Z. *Biomacromolecules* **2012**, *13*, 2429–2438.
- (69) Zhang, Z.; Yin, L.; Tu, C.; Song, Z.; Zhang, Y.; Xu, Y.; Tong, R.; Zhou, Q.; Ren, J.; Cheng, J. *ACS Macro Lett.* **2013**, *2*, 40–44.
- (70) Ryu, J.-H.; Chacko, R. T.; Jiwpanich, S.; Bickerton, S.; Babu, R. P.; Thayumanavan, S. *J. Am. Chem. Soc.* **2010**, *132*, 17227–17235.
- (71) Zhang, Q.; Aleksanian, S.; Noh, S. M.; Oh, J. K. *Polym. Chem.* **2012**, *4*, 351–359.
- (72) Oh, J. K.; Tang, C.; Gao, H.; Tsarevsky Nicolay, V.; Matyjaszewski, K. *J. Am. Chem. Soc.* **2006**, *128*, 5578–5584.
- (73) Matyjaszewski, K.; Xia, J. *Chem. Rev.* **2001**, *101*, 2921–2990.
- (74) Kamigaito, M.; Ando, T.; Sawamoto, M. *Chem. Rev.* **2001**, *101*, 3689–3745.

- (75) *Handbook of Radical Polymerization*; Matyjaszewski, K., Davis, T. P., Eds.; John Wiley & Sons, Inc.: Hoboken, NJ, 2002.
- (76) Chen, W.; Meng, F.; Li, F.; Ji, S.-J.; Zhong, Z. *Biomacromolecules* **2009**, *10*, 1727–1735.
- (77) Huang, X.; Du, F.; Cheng, J.; Dong, Y.; Liang, D.; Ji, S.; Lin, S.; Li, Z. *Macromolecules* **2009**, *42*, 783–790.
- (78) Huynh, V.-T.; de Souza, P.; Stenzel, M. H. *Macromolecules* **2011**, *44*, 7888–7900.
- (79) Liang, H.-F.; Chen, S.-C.; Chen, M.-C.; Lee, P.-W.; Chen, C.-T.; Sung, H.-W. *Bioconjugate Chem.* **2006**, *17*, 291–299.
- (80) Hong, R.; Han, G.; Fernandez, J. M.; Kim, B.-j.; Forbes, N. S.; Rotello, V. M. *J. Am. Chem. Soc.* **2006**, *128*, 1078–1079.
- (81) Oh, J. K.; Siegwart, D. J.; Lee, H.-i.; Sherwood, G.; Peteanu, L.; Hollinger, J. O.; Kataoka, K.; Matyjaszewski, K. *J. Am. Chem. Soc.* **2007**, *129*, 5939–5945.